

REGULAR ARTICLE

Interaction energies and structures of the $\text{Li}^+ \cdot (\text{CO})_n$ ($n = 1-3$) complexes

JAMAL N DAWOUD*

Department of Chemistry, Faculty of Science, Hashemite University, P.O. Box 150459, Zarqa 13115, Jordan
E-mail: jamaldawoud@hu.edu.jo

MS received 14 November 2016; revised 29 March 2017; accepted 8 April 2017

Abstract. The bonding and structures of lithium ion carbonyl complexes, $\text{Li}^+ \cdot (\text{CO})_{1-3}$, were studied at the CCSD and MP2 levels of theories. A linear configuration is formed for the global minimum of the $\text{Li}^+ \cdot \text{CO}$ and $\text{Li}^+ \cdot (\text{CO})_2$ complexes with bond dissociation energies of 13.7 and 12.4 kcal mol⁻¹, respectively. For the $\text{Li}^+ \cdot (\text{CO})_3$ complex, a trigonal planar geometry is formed for the global minimum with a bond dissociation energy of 9.7 kcal mol⁻¹. The computed sequential bond dissociation energies of $\text{Li}^+ \cdot (\text{CO})_n$ ($n = 1-3$) complexes agreed with the experimental findings, in which the electrostatic energy plays an important role in the obtained trend.

Keywords. Lithium ion complexes; *ab initio* calculations; bond dissociation energy; electrostatic interaction; carbon oxide.

1. Introduction

The chemistry of alkali metal interactions with ligands has been the subject of considerable attention in the last twenty years. It has decisive implications in biology, chemistry and physics.¹⁻³ The continuous development in the production of new synthetic adsorbents attract great attention especially for air separation and purification.³⁻⁵ These kinds of technologies are mainly dependent on variations in the strength of interactions among the components of a gas mixture.^{6,7} These studies are very important in atmospheric pollution control, gas sensing and storage.^{7,8} Despite the weak non-covalent bonding interaction, it is important for aggregation of molecules in certain specific configurations and hence governs the behavior of these molecular systems. Alkali metal-ligand complex represents an example of a well known non-covalent bonding interaction.^{9,10}

The interaction of lithium ion with molecular CO has been studied by a number of research groups. In 1974, Toennies *et al.*, had measured the differential cross section for an inelastic scattering of Li^+ ions by N_2 and CO molecules using time-of-flight techniques. The vibration and rotational excitations at low energy collisions for $\text{Li}^+ \cdot \cdot \cdot \text{CO}/\text{N}_2$ complexes were investigated.¹¹ Afterwards, a number of theoretical studies were applied to investigate the potential energy sur-

face of $\text{Li}^+ \cdot \cdot \cdot \text{CO}$ complex using SCF,¹² HF and MP2 calculations.¹³ Briefly, these calculations showed the existence of two minima and one transition state. In addition, the Li^+ ion is preferred to bind with C-atomic site rather than O-atomic site in a linear configuration.

In the nineties, the alkali ion carbonyl complexes have been revisited experimentally in detail. The sequential bond dissociation energies of the $\text{Li}^+ \cdot (\text{CO})_n$ ($n = 1-3$) complexes were determined by means of guided ion beam mass spectrometry and these complexes followed a specific trend.^{10,14} The adsorption of CO molecules on a series of Li-EMT zeolite at 85 K has been invoked using FTIR spectroscopy.¹⁵ These results showed that the linear structures of $\text{Li}^+ - \text{CO}$ complex exhibit two CO vibration frequencies, $\nu_{\text{C=O}}$, at 2183 cm⁻¹ and 2140 cm⁻¹. In addition, a peak at $\nu_{\text{C}\equiv\text{O}}$ of 2166 cm⁻¹ was attributed to $\text{Li}^+ \cdot (\text{CO})_2$ complex. Recently, the adsorption of CO on Li-exchanged zeolites (Li-ZSM-5) were examined using variable temperature infrared spectroscopy (VTIR) accompanied by DFT calculations.⁶ This study was applied to calculate the thermodynamic quantities, ΔH and ΔS , of the adsorption process and show the consistency of the VTIR measurements with the reported calorimetric results of the $\text{Li}^+ \cdot \cdot \cdot \text{CO}$ complexation. The interaction energy of Li^+ ion with CO molecule was calculated on the basis of B3LYP/VDZP method. In these calculations, different embedding cluster models of cationic zeolite sites were used.

*For correspondence

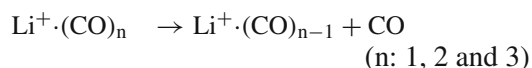
It is worth mentioning that none of these theoretical calculations deal with the potential energy surface (PES) and the binding energy of more than a single CO molecule bonded to Li^+ ion. Therefore, the aim of the present study is to construct and determine the PES, structures of $\text{Li}^+(\text{CO})_{1-3}$ complexes and explain the variation in the sequential bond energies of these complexes.

2. Computational details

The geometries of all the complexes included in this study are fully optimized at the CCSD and MP2 levels of theories using the Gaussian 03 program.¹⁶ These calculations were performed using different types of polarization and diffused basis sets such as 6-31+G(d) and 6-311+G(d). These kinds of basis sets are appropriate to construct the potential energy surface and to optimize the geometries of the $\text{Li}^+(\text{CO})_{1-3}$ complexes.

On the potential energy surface, all stationary points, minima or transition states, have been confirmed using intrinsic reaction coordinate (IRC) method by calculating harmonic vibrational frequencies of the titled $\text{Li}^+(\text{CO})_{1-3}$ complexes.^{17,18} Furthermore, the electronic and zero point energy (ZPE) for each stationary point were calculated at $T = 298$ K. The binding energy was calculated from the difference between the total electronic energy, corrected for finite temperature, of the complex minus the electronic energies of the un-complexed Li^+ ion and CO molecule. The calculated binding energy was then corrected for basis set superposition error (BSSE) using the full counterpoise method.^{19,20}

The successive sequential bond dissociation energies of the $\text{Li}^+(\text{CO})_n$ complexes were calculated at different orientations for the global minima states according to the following equation:



To explain and understand the experimental trend of the sequential bond dissociation energies, the $\text{Li}^+ \cdots \text{CO}$ bond order (BO), natural electronic configurations and the atomic charge distributions of the $\text{Li}^+(\text{CO})_n$ complex for different structures were calculated, according to the NBO analysis. The calculated charge distribution spread over an atom was treated as a point charge located at that atom in the complex as applied elsewhere.²¹⁻²⁴ Using these point charges, the electrostatic contribution, $E_{elec.}$, to the bond dissociation energy of the $\text{Li}^+(\text{CO})_n$ complex was calculated as a pair-wise sum of point charges placed at each atomic site of CO and Li^+ ion using the following formula,

$$E_{elec.} = -\frac{q_{Li}}{4\pi\epsilon_0 n} \sum_{n=1}^3 \left(\frac{q_C}{r_{Li-C}} + \frac{q_O}{r_{Li-O}} \right) \quad (1)$$

where, n is the number of CO molecules in the complex, q_{Li} , q_C and q_O are their point charges located on Li^+ , C and O

sites, respectively. $r_{Li-C/O}$ is the distance between the Li^+ ion and atomic C/O in the complex. ϵ_0 is the permittivity of the vacuum.

3. Results and Discussion

3.1 $\text{Li}^+\cdot\text{CO}$ complex

The intrinsic reaction coordinate of the $\text{Li}^+\cdot\text{CO}$ complex ($^1\Sigma^+$), performed at the MP2 level of theory, showed the existence of one transition (T-shaped) and two minima (linear structure, in which the Li^+ ion interacts with each end of the CO molecule) states, as shown in Figure 1. The optimized geometrical parameters of the $\text{Li}^+\cdot\text{CO}$ complexes are given in Table 1. For the CCSD and MP2 methods, the results of the calculated parameters are consistent and in good agreement. The global minimum is formed when the Li^+ ion is directly bonded to the C-atomic site at a distance of $r_{(\text{Li}-\text{C})} = 2.236 \text{ \AA}$ and $r_{(\text{C}-\text{O})} = 1.132 \text{ \AA}$ [calculated on the basis of the CCSD/6-31+G(d)], which agreed well with many reported results of theoretical calculations that yielded similar geometrical parameters (see Table 1).^{12,13} Our best value, the closest to experimental findings, of the CO bond length agreed well with the bond length of free CO molecule.²⁵ The other local minimum is formed when the Li^+ ion is directly bonded with O-atomic site at a distance of $r_{(\text{Li}-\text{O})} = 1.978 \text{ \AA}$ and $r_{(\text{C}-\text{O})} = 1.143 \text{ \AA}$ [calculated on the basis of the CCSD/6-311+G(d)], which is slightly longer than that of the free CO bond length. The frequency calculations of the $\text{Li}^+\cdot\text{CO}$ complex, for its minima structures, show that the best values exist at 2313 cm^{-1} (Li^+-CO) and 2130 cm^{-1} (Li^+-OC) and in good agreement with 2532 cm^{-1} that was measured experimentally for Li^+-CO complex in gas phase.¹⁴ Furthermore, these results, calculated using the CCSD/6-311+G(d) method, agree well with the experimental values of 2183 cm^{-1} and 2140 cm^{-1} for $\text{Li}^+\cdot\text{CO}$ complex.¹⁵ The T-shaped structure of the complex is found to be a transition state and its structural parameters are shown in Table 1.

The binding energy values were calculated, including zero-point energy (ZPE) and BSSE correction, for the local and global minima structures at the levels of CCSD and MP2 using 6-311+G(d) basis set function. These results are listed in Table 2. Interestingly, the CCSD and MP2 calculations of the binding energy are close to each other, indicating that these results are consistent for $\text{Li}^+\cdot\text{CO}$ complex. Our best value for the binding energy of the linear structure, $\text{Li}^+ - \text{CO}$, was calculated and found to be $13.7 \text{ kcal mol}^{-1}$, which is

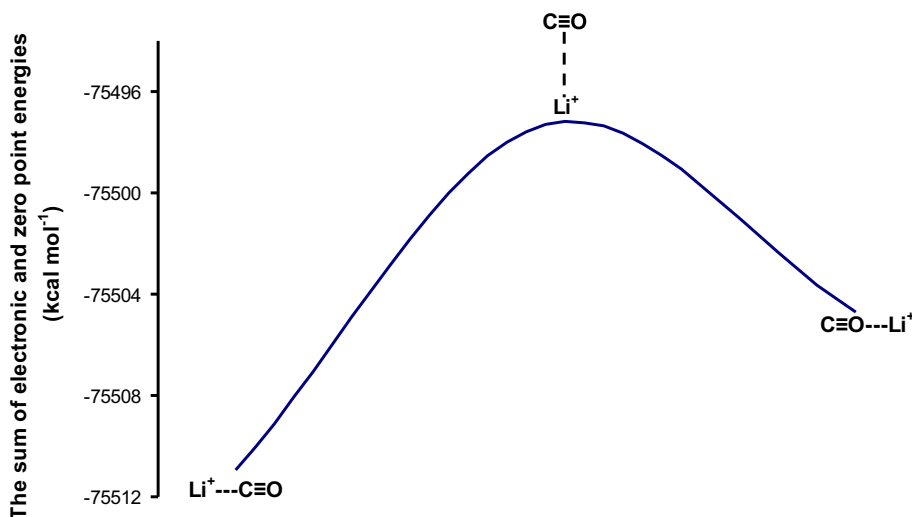


Figure 1. The IRC schematic diagram represents the potential energy surface of $\text{Li}^+\cdot\text{CO}$ adducts calculated on the basis of MP2/6-311+G(d) method.

Table 1. Geometrical parameters of the $\text{Li}^+\cdot\text{CO}$ complex^a for different configurations.

Geometry	Method	Basis set	$r_{(\text{C}-\text{O})}$	$r_{(\text{Li}-\text{C})}$	$r_{(\text{Li}-\text{O})}$	$\theta(^{\circ})^b$	$\theta(^{\circ})^c$
Linear $\text{Li}^+\cdot\text{CO}$	CCSD	6-31+G(d)	1.132	2.236	–	180.0	–
		6-311+G(d)	1.121	2.206	–	180.0	–
Free CO	MP2	6-311+G(d)	1.131	–	–	–	–
		6-31+G(d)	1.143	2.229	–	180.0	–
Free CO	SCF ^d	6-311+G(d)	1.132	2.200	–	180.0	–
		6-311+G(d)	1.140	–	–	–	–
		Huzinaga basis set	1.128	2.272	–	180.0	–
Linear $\text{Li}^+\cdot\text{OC}$	HF ^e	6-21G	1.129	2.213	–	180.0	–
		6-31+G(d)	1.154	–	1.982	–	180.0
Linear $\text{Li}^+\cdot\text{OC}$	CCSD	6-311+G(d)	1.143	–	1.978	–	180.0
		6-31+G(d)	1.159	–	2.013	–	180.0
Linear $\text{Li}^+\cdot\text{OC}$	MP2	6-311+G(d)	1.149	–	2.008	–	180.0
		6-31+G(d)	1.149	–	2.008	–	180.0
Linear $\text{Li}^+\cdot\text{OC}$	SCF ^d	Huzinaga basis set	1.128	–	1.903	–	180.0
Linear $\text{Li}^+\cdot\text{OC}$	HF ^e	6-21G	1.129	–	1.836	–	180.0
T-shaped TS	CCSD	6-31+G(d)	1.143	2.566	–	82.1	–
		6-311+G(d)	1.132	2.511	–	80.9	–
	MP2	6-31+G(d)	1.154	2.591	–	77.0	–
		6-311+G(d)	1.143	2.543	–	75.7	–
T-shaped TS	SCF ^d	Huzinaga basis set	1.128	2.801	–	75.0	–

^aAll the bond lengths are in Å, and the bond angles are in degrees. ^b $\angle \text{Li-C1-O2}$ bond angle. ^c $\angle \text{Li-O2-C1}$ bond angle. ^dTaken from ref. ¹². ^eTaken from ref. ¹³.

in an excellent agreement with the experimental value, $13.2 \pm 3.1 \text{ kcal mol}^{-1}$, that was measured using ion beam mass spectrometer technique.^{10,14}

Table 2 reports that our calculations agreed well with previous SCF and HF results calculated by Steammler,¹² and Del Bene *et al.*¹³ The binding energy of the local minimum structure, $\text{Li}^+ - \text{OC}$, is less than that of the global minimum by $\sim 3.0 \text{ kcal mol}^{-1}$ (on the basis of CCSD results) and $5.0 \text{ kcal mol}^{-1}$ (on the basis of MP2 results). These results agree well with a binding energy

of $11.7 \text{ kcal mol}^{-1}$ that was calculated for the local minimum using HF/6-31G* method (see Table 2).¹³

The natural bond orbital (NBO) analysis of the atomic charge distribution of the $\text{Li}^+\cdot\text{CO}$ complexes show that Li^+ ion still retains most of its positive charge in linear and T-shaped structures (see Figure 2). These results confirm the electrostatic nature of the bonding interactions in these complexes. For CO molecule, the C atom will gain electrons from $\sigma_{\text{C-O}}$ bond and at the same time it will lose the electron lone pair on C atom to the

Table 2. Binding energy (BE) and BSSE values for the $\text{Li}^+\cdot(\text{CO})_{1-3}$ complexes, at the levels of CCSD and MP2 methods.

Structure	Symmetry	Method	Basis set	BE	BSSE
Linear $\text{Li}^+\cdot\text{CO}$	$C_{\infty v}$	CCSD	6-311+G(d)	13.7	0.57
		MP2	6-311+G(d)	15.1	0.53
		Expt. ^a	–	13.2 ± 3.1	–
		SCF ^b	Huzinaga basis set	14.3	–
		HF ^c	6-31G*	17.4	–
Linear $\text{Li}^+\cdot\text{OC}$	$C_{\infty v}$	CCSD	6-311+G(d)	10.7	0.96
		MP2	6-311+G(d)	9.8	0.87
		HF ^c	6-31G*	11.5	–
$\text{Li}^+(\text{CO})_2$ (A)	$D_{\infty h}$	CCSD	6-311+G(d)	26.4	1.50
		MP2	6-311+G(d)	28.3	1.42
$\text{Li}^+(\text{CO})(\text{OC})$ (B)	$C_{\infty v}$	CCSD	6-311+G(d)	23.5	2.00
		MP2	6-311+G(d)	22.8	1.85
$\text{Li}^+(\text{OC})_2$ (C)	$D_{\infty h}$	CCSD	6-311+G(d)	20.4	2.50
		MP2	6-311+G(d)	17.3	2.60
$\text{Li}^+(\text{CO})_3$ (D)	D_{3h}	CCSD	6-311+G(d)	35.3	2.27
		MP2	6-311+G(d)	37.8	2.15
$\text{Li}^+(\text{CO})_2(\text{OC})$ (E)	C_{2v}	CCSD	6-311+G(d)	33.8	2.68
		MP2	6-311+G(d)	34.9	2.49
$\text{Li}^+(\text{CO})(\text{OC})_2$ (F)	C_{2v}	CCSD	6-311+G(d)	31.6	3.15
		MP2	6-311+G(d)	29.1	2.97
$\text{Li}^+(\text{OC})_3$ (G)	D_{3h}	CCSD	6-311+G(d)	28.5	3.64
		MP2	6-311+G(d)	25.3	3.36

The units are in kcal mol⁻¹

^aTaken from ref. 10

^bTaken from ref. 12

^cTaken from ref. 13.

$\pi_{\text{C-O}}$ bond, C atom will loose more than it gains. This creates a net positive charge on C and a net negative charge on O at equilibrium as predicted elsewhere.²⁵ On the other hand, the electrostatic potential (EP) map shows that both C and O ends have negative electrostatic potential with O site exhibiting more negative EP (see Figure 2b). In the proximity of C/O nuclei, a positive EP is observed and C atomic site has larger positive EP. This behavior is attributed to the short CO bond length which pushes the electron population of triple bond outside the C and O nuclei. This intriguing EP of CO molecule was recently studied in detail and our results agreed well with previous MP2 calculations findings.²⁶

Compared to atomic charges of naked molecular CO, it was found that the non-bonding and bonding electrons of CO moiety, in global minimum, are highly polarized. The positive charge of the carbon atom nearest to Li^+ ion is decreased by 0.122, whereas the negative charge of the oxygen atom, the farthest from Li^+ ion, is also reduced by 0.166. This confirms a migration of electronic charge from oxygen to carbon in CO moiety as a result of attraction forces with Li^+ ion. For the local minimum structure, $\text{Li}^+ - \text{OC}$, the

situation is completely reversed where a migration of electrons from carbon atom, the farthest from Li^+ ion, to oxygen atom, the closest to Li^+ ion, occurred as a result of attractive forces between them. It is worthy to mention here that CO bond in $\text{Li}^+ - \text{OC}$ is lengthened by $\sim 0.015 \text{ \AA}$ as a result of migration of the electrons from non-bonding orbitals to anti-bonding orbitals, π_{2p}^* and σ_{2p}^* , and hence increases the bond length. This kind of behavior is consistent with the results of HF/6-31G* calculation of $\text{Li}^+ \cdot \text{CO}$ complex¹³ and recent theoretical results of the $\text{Cu}^+ \cdot \text{CO}$ complex.²³

3.2 The $\text{Li}^+ \cdot (\text{CO})_2$ and $\text{Li}^+ \cdot (\text{CO})_3$ complexes

The geometries of $\text{Li}^+ \cdot (\text{CO})_2$ and $\text{Li}^+ \cdot (\text{CO})_3$ complexes, in ground state of PES, were optimized and the results are shown in Figures 3 and 4, respectively. The IRC test accompanied with frequency calculations show that the $\text{Li}^+ \cdot (\text{CO})_2$ complex has three minima of linear configurations and two transition states of T-shaped structures, as presented in Figure 5. The global minimum, structure **A**, is formed when the Li^+ ion is bonded with each carbon atomic site located on the two CO molecules,

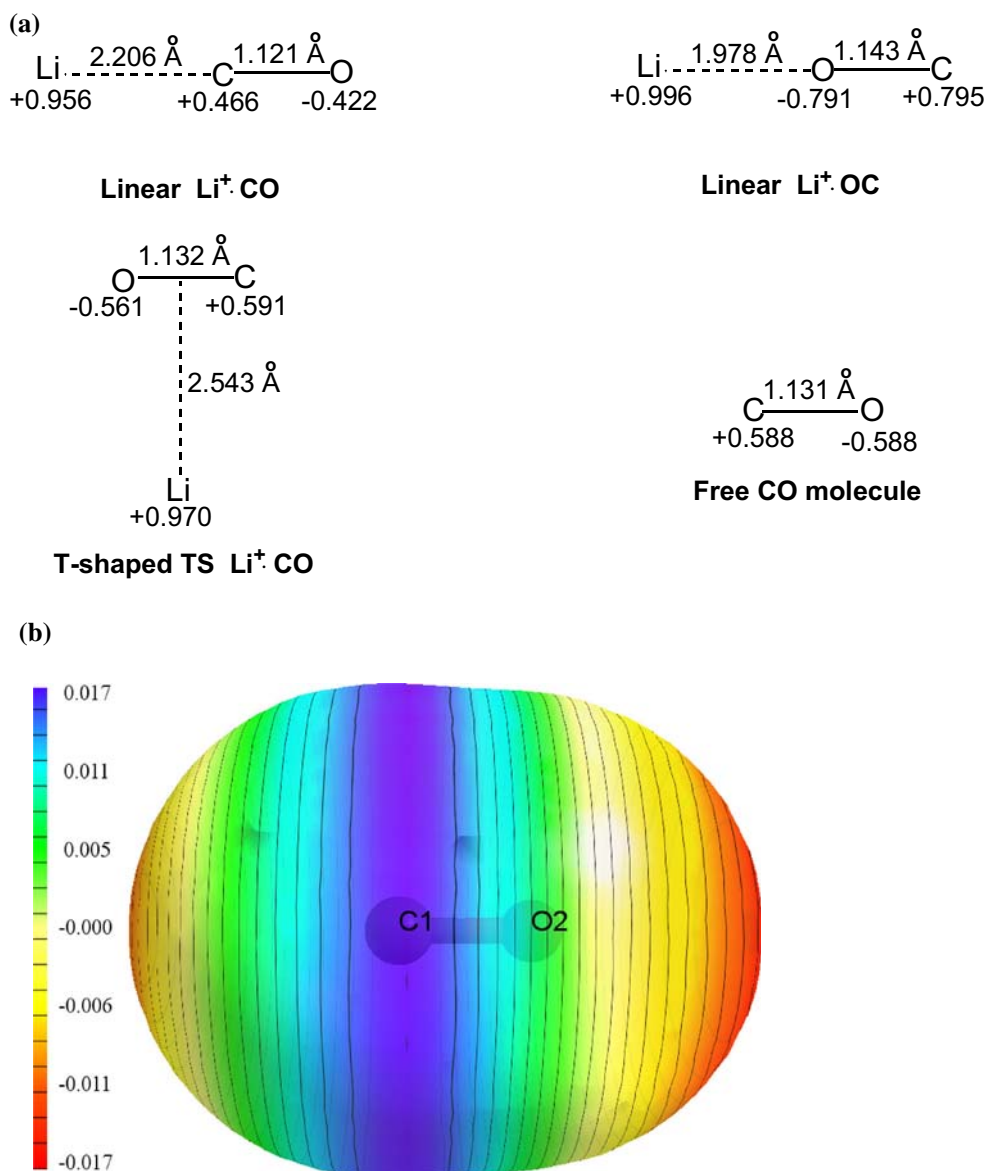


Figure 2. (a) NBO analysis of the atomic charge distributions of free CO molecule and $\text{Li}^+\cdot\text{CO}$ complex for different configurations obtained on the basis of the CCSD/6-311+G(d) method. (b) The electrostatic potential map of CO molecule calculated on the basis of CCSD/6-311+G(d) method.

whereas the other two local minima exhibit the same configuration. The first one, structure **B**, is formed when the Li^+ ion is bonded with C and O sites located on two different CO molecules. The second one, structure **C**, is obtained when the Li^+ ion is bonded directly with two O atomic sites on two CO molecules. These structures are listed in Figure 3.

Figure 6 presents the IRC results of the potential energy surface of the $\text{Li}^+\cdot(\text{CO})_3$ complex. The results of CCSD and MP2 calculations show the existence of four minima and three transition state structures. The global minimum, structure **D**, is formed when the Li^+ ion is directly bonded with each C-atomic site of three

CO molecules in a trigonal planar structure (see Figure 4). For the other three local minima, the Li^+ ion was bonded with C and O atomic sites of different CO molecules in a trigonal planar geometry (**E** and **G** structures, see Figure 4). For structure **F**, the Li^+ ion is bonded with two oxygens and single carbon atomic sites placed on three different CO molecules which yielded a trigonal planar of C_{2v} symmetry. In addition, Figure 4 shows that the $\text{Li}^+\cdot(\text{CO})_3$ complex exhibits a **Y**-shaped structure for the three transition states.

The binding energy of the carbonyl lithium ion complexes, in which the Li^+ ion bonded with two to three

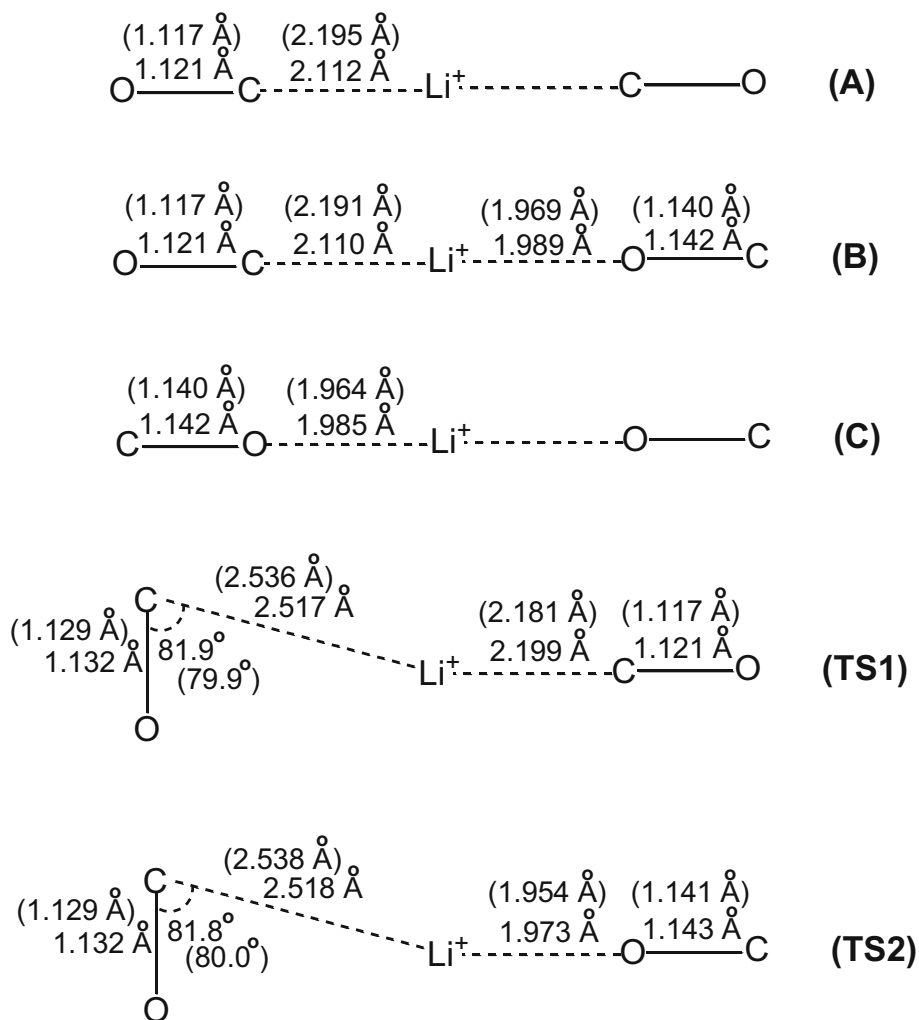


Figure 3. The optimized structures for the minima and transition states of the $\text{Li}^+(\text{CO})_2$ complex that were obtained on the basis of the CCSD/6-311+G(d) method. The MP2/6-311+G(d) results are listed in brackets.

CO ligands, has been calculated and listed in Table 2. These calculations indicate a strong tendency for C-atomic site of CO molecule to bind with Li^+ ion. Obviously, the binding energy of these complexes at different configurations increases linearly with the number of carbon atomic sites bonded to Li^+ ion. As shown in Table 2, the binding energy values calculated on the basis of the MP2 and CCSD methods are consistent with slight variation in the binding energy values of $\sim 2.6 \text{ kcal mol}^{-1}$ for structures **D** and **G**. However, the results still agreed well with each other and yielded the same trend.

3.3 Sequential bond energies of $\text{Li}^+(\text{CO})_n$ ($n: 1-3$)

The sequential bond dissociation energies (BDEs) of $\text{Li}^+(\text{CO})$, $\text{Li}^+(\text{CO})_2$ and $\text{Li}^+(\text{CO})_3$ at their global

minimum configurations were calculated at the CCSD and MP2 levels of theories. These results are listed in Table 3. These calculations show that the BDEs follow the ordering, $\text{Li}^+(\text{CO}) > \text{Li}^+(\text{CO})_2 > \text{Li}^+(\text{CO})_3$. This is consistent with the $\text{Li}^+ - \text{C}$ bond order (BO) values where the mono ligated complex exhibits the largest BO value and hence it has the strongest $\text{Li}^+ - \text{CO}$ interaction (see Figure 7). These results agree very well with the experimental findings.^{10,14} Table 3 shows that the CCSD values of BDEs are better than those obtained by MP2 methods and closer to the experimental findings. However, the best value of the calculated BDE for the $\text{Li}^+(\text{CO})_2$ structure is still larger than the upper limit of the experimental value by $2.8 \text{ kcal mol}^{-1}$.

To clarify the trend of the sequential bond dissociation energies that was observed experimentally, the NBO

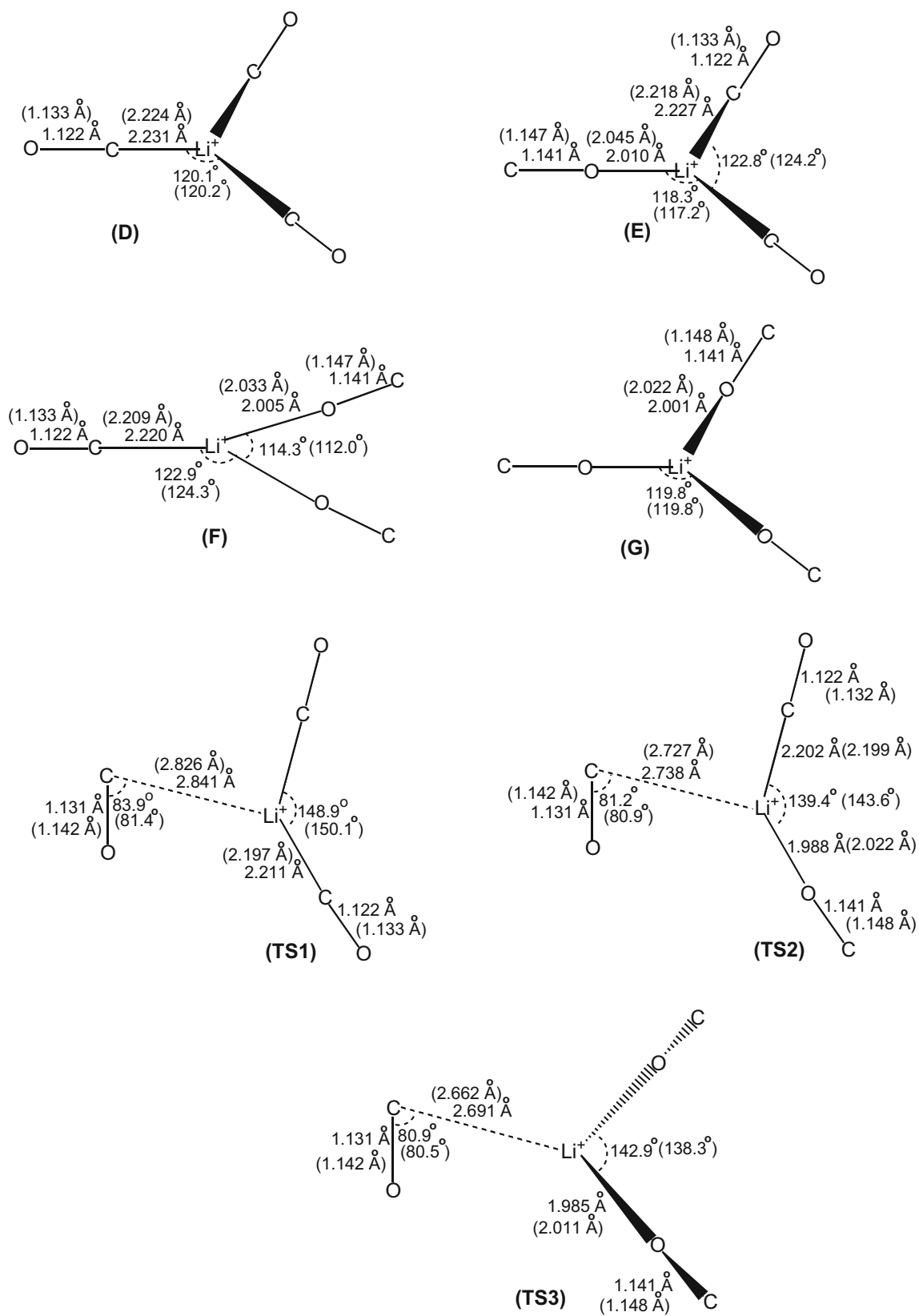


Figure 4. The optimized structures for the minima and transition states of the $\text{Li}^+(\text{CO})_3$ complex that were obtained on the basis of the CCSD/6-311+G(d) method. The MP2/6-311+G(d) results are listed in brackets.

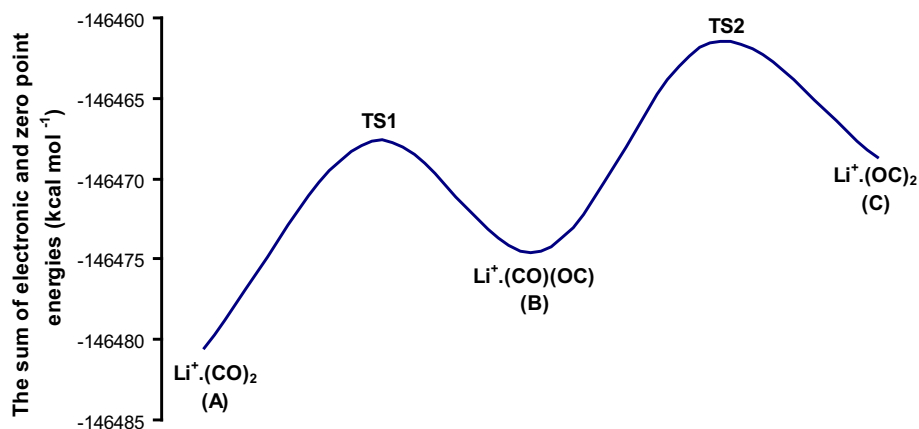


Figure 5. The IRC schematic diagram represents the potential energy surface of $\text{Li}^+(\text{CO})_2$ complex calculated on the basis of MP2/6-311+G(d) method.

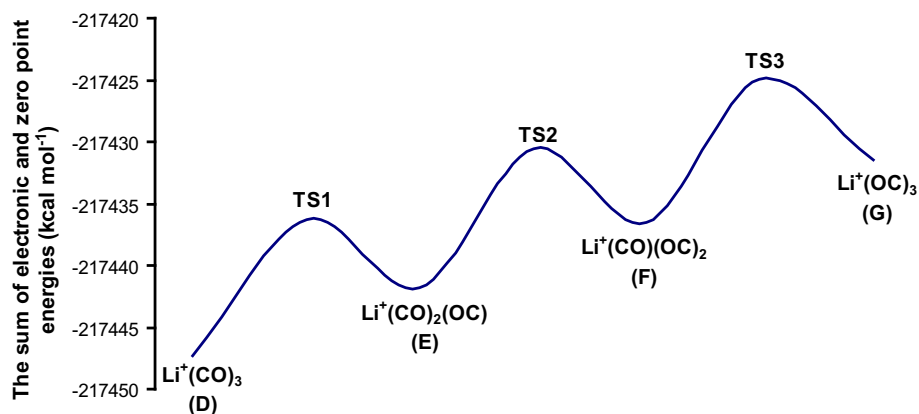


Figure 6. The IRC schematic diagram of the $\text{Li}^+(\text{CO})_3$ complex generated at the MP2/6-311+G(d) level of theory.

Table 3. Sequential bond dissociation energies (BDE) of the global minimum structures of the $\text{Li}^+(\text{CO})_n$ complexes ($n: 1-3$), calculated at the levels of the CCSD and MP2 methods. The units are in kcal mol^{-1} .

Structure	Method	Basis set	BDE	BSSE
The $\text{Li}^+\text{-CO}$ complex				
Linear $\text{Li}^+\text{-CO}$	CCSD	6-311+G(d)	13.7	0.57
	MP2	6-311+G(d)	15.1	0.53
	Expt. ^a	–	13.2 ± 3.1	–
The $\text{Li}^+(\text{CO})_2$ complex				
Linear $(\text{CO})\cdot\text{Li}^+\text{-CO}$	CCSD	6-311+G(d)	12.4	1.15
	MP2	6-311+G(d)	13.5	1.10
	Expt. ^a	–	8.6 ± 1.0	–
The $\text{Li}^+(\text{CO})_3$ complex				
Trigonal planar $(\text{CO})_2 \cdot \text{Li}^+\text{-CO}$	CCSD	6-311+G(d)	9.1	1.07
	MP2	6-311+G(d)	10.0	1.03
	Expt. ^a	–	8.3 ± 1.0	–

^aTaken from ref. ¹⁰.

analysis of atomic charge distributions of $\text{Li}^+(\text{CO})_{1-3}$ for the global minima configurations were calculated on the basis of the CCSD/6-311+G(d) method and listed in

Figure 7. The geometrical parameters with their atomic charges were used to calculate the electrostatic energy contribution to the bond dissociation energy using equa-

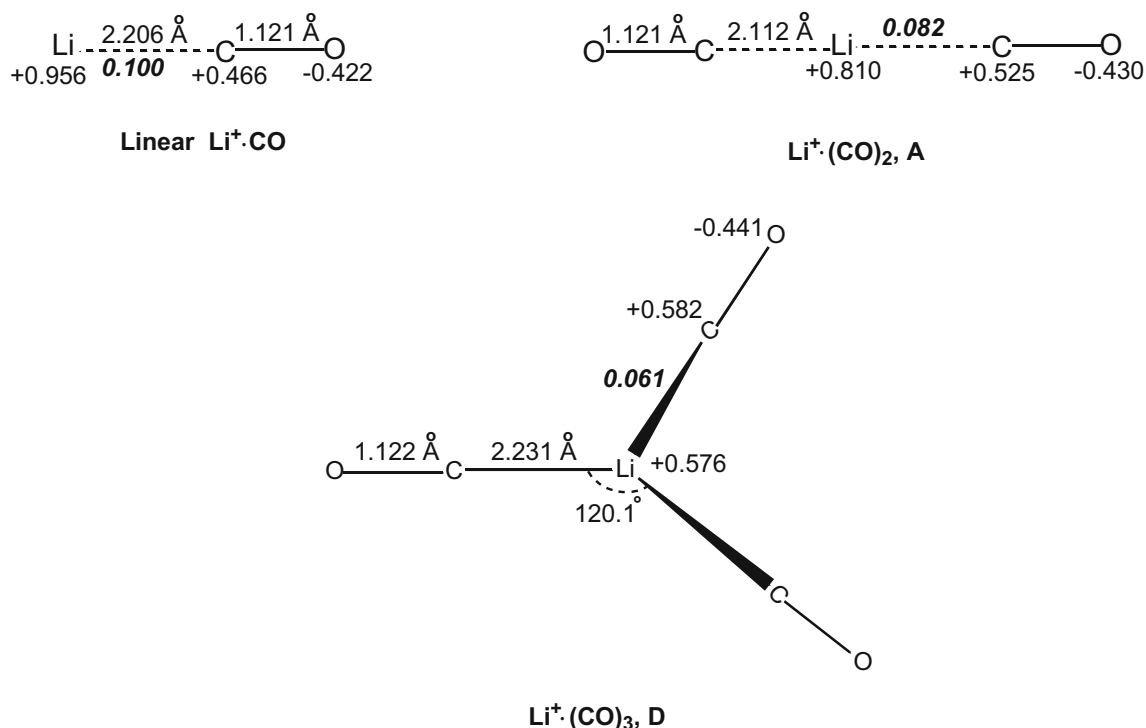


Figure 7. The NBO analysis of the atomic charge distributions of the $\text{Li}^+\cdot(\text{CO})_n$ complexes ($n = 1-3$) calculated on the basis of the CCSD/6-311+G(d) method. The bond order values are given in bold italic numbers.

tion (1). These results are presented in Table 4. The values of the electrostatic energy were found to follow the same trend as those obtained for the BDEs, in which

Table 4. The electrostatic contribution, $E_{elec.}$, to the bond dissociation energies of the CO complexes, $\text{Li}^+\cdot(\text{CO})_n$ ($n = 1-3$), in gas phase, calculated on the basis of the CCSD/6-311+G(d) method.

Structure	$E_{elec.}$ (kcal mol ⁻¹)
Linear $\text{Li}^+\cdot\text{CO}$	-67.15
Linear $\text{Li}^+\cdot(\text{CO})_2$	-66.83
Trigonal planar $\text{Li}^+\cdot(\text{CO})_3$	-49.95

the electrostatic energy is decreased with the number of CO molecules, as a result of decreasing the charge on the Li^+ and the closest carbon atomic site of the CO molecule to the ion (Figure 7). This will reduce the interaction forces within these complexes, mainly in terms of electrostatic energy. In addition, the NBO analysis of electronic configuration of these complexes were determined and listed in Table 5. These results show that the electronic population migrates from oxygen to carbon atom within CO accompanied with electronic charge transfer from CO molecule toward the Li^+ ion, particularly in di- and tri-ligated complexes. This is reflected in decreasing of the Li cationic charge and the obtained BDEs trend.

Table 5. Results of NBO analysis of the natural electronic configuration of the global minima structures of the $\text{Li}^+\cdot(\text{CO})_n$ complexes ($n: 1-3$), calculated at the level of the CCSD/6-311+G(d) method.

Complex	Natural electronic configuration		
	Li	C	O
CO	-	[core] $2s^{1.61} 2p^{1.74}$	[core] $s^{1.73} 2p^{4.84}$
Linear $\text{Li}^+\cdot\text{CO}$	[core] $s^{0.02} 3p^{0.02}$	[core] $2s^{1.51} 2p^{1.96}$	[core] $2s^{1.71} 2p^{4.70}$
Linear $\text{Li}^+\cdot(\text{CO})_2$	[core] $2s^{0.10} 3p^{0.08}$	[core] $2s^{1.49} 2p^{1.93}$	[core] $2s^{1.71} 2p^{4.71}$
Trigonal planar $\text{Li}^+\cdot(\text{CO})_3$	[core] $2s^{0.20} 3p^{0.22}$	[core] $2s^{1.46} 2p^{1.90}$	[core] $2s^{1.71} 2p^{4.72}$

4. Conclusions

In this work, a computational study of lithium ion carbonyl complexes within CCSD and MP2 methods was performed. For the $\text{Li}^+\cdot(\text{CO})$ and $\text{Li}^+\cdot(\text{CO})_2$ complexes, a linear structure was obtained for the global and local minima, whereas a T-shaped structure was adopted for all transition states. For the $\text{Li}^+\cdot(\text{CO})_3$, trigonal planar geometry were obtained for the global minimum, structure **D** with a D_{3h} symmetry, and C_{3v} and D_{3h} symmetries for all other local minima structures **E**, **F** and **G**. In addition, all transition states of the tri-ligated complex adopted Y-shaped structure. The agreement of the calculated BDEs according to eq. (1) and the reported experimental data as well as other theoretical calculations is excellent for these Li ion complexes.

The sequential bond dissociation energies (BDE) of the lithium ion carbonyl complexes show a specific trend where the mono ligated complex has the strongest BDE. This trend is highly dependent on the electrostatic interaction energy in these complexes.

Acknowledgements

JND would like to thank the Deanship of Research and Graduate Studies at the Hashemite University (Jordan) for the financial support.

References

- Jensen F 1992 Structure and stability of complexes of glycine and glycine methyl analogs with H^+ , Li^+ and Na^+ *J. Am. Chem. Soc.* **114** 9533
- Ai H, Bu Y, Li P, Chen Z and Hu X 2004 Structure and positive binding energies of glycine-2Li⁺ in the gas phase: A theoretical study on optimal reaction pathway and proton transfer induced by two lithium cations *J. Mol. Struct. THEOCHEM* **678** 91
- Yang R T 1987 *Gas Separation by Adsorption Processes* (Boston: Butterworths)
- Lavalley J C 1996 Infrared spectrometric studies of the surface basicity of metal oxides and zeolites using adsorbed probe molecules *Catal. Today* **27** 377
- Jüntegn H 1977 New applications for carbonaceous adsorbents *Carbon* **15** 273
- Areán C O, Nachtigallová D, Nachtigall P, Garrone E and Delgado M R 2007 Thermodynamics of reversible gas adsorption on alkali-metal exchanged zeolites-the interplay of infrared spectroscopy and theoretical calculations *Phys. Chem. Chem. Phys.* **9** 1421
- Reiss G 1994 Status and development of oxygen generation process on molecular sieve zeolites *Gas Sep. Purif.* **8** 95
- Chu X Z, Zhou Y P, Zhang Y Z, Su W, Sun Y and Zhou L 2006 Adsorption of hydrogen on micro- and mesoporous adsorbents with orderly structure *J. Phys. Chem. B* **110** 22596
- Budenholzer F E, Gislason E A and Jorgensen A D 1986 Determination of potassium ion-small-molecule potentials from total cross section measurements *Chem. Phys.* **110** 171
- Rogers M T and Armentrout P B 2000 Noncovalent metal-ligand bond energies as studied by threshold collision-induced dissociation *Mass Spectrom. Rev.* **19** 215
- Levine R D, Bernstein R B, LaBudde R A, Böttner R, Ross U, Toennies J P, King D L, Loesch H J, Herschbach D R, Ding A M G, Polanyi J C, Kendall G M, Larsen R A, krenos J R and Aquilanti V 1973 General discussion *Faraday Discuss. Chem. Soc.* **55** 221
- Steammmler V 1976 Ab initio calculation of the potential energy surface of the system Li^+/CO *Chem. Phys.* **17** 187
- Del Bene J E, Frisch M J, Raghavachari K, Pople J A and Schleyer P v R 1983 A molecular orbital study of some lithium ion complexes *J. Phys. Chem.* **87** 73
- Walter D, Seviens M R and Armentrout P B 1998 Alkali ion carbonyls: Sequential bond energies of $\text{Li}^+(\text{CO})_x$ ($x = 1-3$), $\text{Na}^+(\text{CO})_x$ ($x = 1, 2$) and $\text{K}^+(\text{CO})$ *Int. J. Mass Spectrom. Ion Processes* **175** 93
- Hadjiivanov K, Massiani P and Knözinger H 1999 Low temperature CO and $^{15}\text{N}_2$ adsorption on alkali cation exchanged EMT zeolites: An FTIR study *Phys. Chem. Chem. Phys.* **1** 3831
- Frisch M *et al.* 2003 *Gaussian 03, Revision B.05*, Pittsburgh: Gaussian, Inc.
- Gonzalez C and Schlegel H B 1989 An improved algorithm for reaction path following *J. Chem. Phys.* **90** 2154
- Gonzalez C and Schlegel H B 1990 Reaction path following in mass-weighted internal coordinates *J. Phys. Chem.* **94** 5523
- Simon S, Duran M and Dannenberg J J 1996 How does basis set superposition error change the potential surfaces for hydrogen-bonded dimers *J. Chem. Phys.* **105** 11024
- Boys S F and Bernardi F 1970 The calculation of small molecular interactions by the differences of separate total energies: Some procedures with reduced errors *Mol. Phys.* **19** 553
- Liu D, Wyttenbach T and Bowers M T 2004 Hydrogen of protonated primary amines: Effects of intermolecular and intramolecular hydrogen bonds *Int. J. Mass Spectrom.* **236** 81
- Dawoud J N, Fafous I I and Harahsheh T K 2014 Structure and potential energy surface of $\text{Na}^{+/0}\cdot(\text{O}_2)_n$ ($n = 1-3$) complexes *Comput. Theor. Chem.* **1027** 62
- Fafous I I, Dawoud J N, Sallabi A K and Hassouneh T S 2015 Adensity functional theory study of the $\text{Cu}^+\cdot(\text{CO})_n$ ($n = 1-3$) complexes *J. Coord. Chem.* **68** 1528
- Dawoud J N 2014 Sequential bond energies and the structures of $\text{Cr}^+\cdot(\text{N}_2)_n$, ($n = 1-4$) *J. Chem. Sci.* **126** 1743
- Harrison J 2006 Relationship between the Charge Distribution and Dipole Moment Functions of CO and the Related Molecules CS, SiO, and SiS *J. Phys. Chem. A* **110** 10848
- Kim H, Doan V, Cho W, Valero R, Tehrani Z, Madrdejós J and Kim K 2015 Intriguing Electrostatic Potential of CO: Negative Bond-ends and positive Bond-cylindrical-surface *Sci. Rep.* **5** 16307